

Nonlocal Landau theory of the magnetic phase diagram of highly frustrated magnetoelectric CuFeO_2

M. L. Plumer

Department of Physics and Physical Oceanography, Memorial University, St. John's, Newfoundland, Canada A1B 3X7

(Received 5 June 2008; revised manuscript received 5 August 2008; published 4 September 2008)

A nonlocal Landau-type free-energy functional of the spin density is developed to model the large variety of magnetic states, which occur in the magnetic-field–temperature phase diagram of magnetoelectric CuFeO_2 . Competition among long-range quadratic exchange, biquadratic antisymmetric exchange, and trigonal anisotropy terms, consistent with the high-temperature rhombohedral $R\bar{3}m$ crystal symmetry, are shown to all play important roles in stabilizing the unusual combination of commensurate and incommensurate spin structures in this highly frustrated triangular antiferromagnet. It is argued that strong magnetoelastic coupling is largely responsible for the nonlocal nature of the free energy. A key feature of the analysis is that an electric polarization is induced by a canting of the noncollinear incommensurate spin structure. Application of the model to ordered spin states in the triangular antiferromagnets MnBr_2 and NaFeO_2 is also discussed.

DOI: [10.1103/PhysRevB.78.094402](https://doi.org/10.1103/PhysRevB.78.094402)

PACS number(s): 75.30.Kz, 75.50.Ee, 75.80.+q, 75.40.Cx

I. INTRODUCTION

One of the more intriguing features of the magnetic-field–temperature (H - T) phase diagram of the rhombohedrally stacked triangular antiferromagnetic (AF) CuFeO_2 is the occurrence of a field-induced noncollinear incommensurate (IC) spin structure among a multitude of commensurate collinear magnetic ordered states.^{1–6} Usual Hund's rules suggest that the magnetic Fe^{3+} ions in this semiconductor do not exhibit low-order spin-orbit coupling since $L=0$ (with $S=5/2$). The origin of the observed c -axis magnetic anisotropy is not precisely understood but it is generally agreed that it should be very weak.^{7,8} The frustration inherent in triangular antiferromagnets is known to give rise to period-3 (P3) elliptically or helically polarized (S) spin structures at $H=0$. A field applied along the anisotropy (\mathbf{c}) direction typically induces a spin-flop transition $\mathbf{S} \perp \mathbf{c}$ in weak axial antiferromagnets.^{9–12} In the case of CuFeO_2 , spin noncollinearity occurs only at moderate values of H , and high-field spin states are linearly polarized with $\mathbf{S} \parallel \mathbf{c}$. A key to the understanding of these unusual features is the very high degree of frustration resulting from not only the triangular geometry but also the long-range exchange interactions, magnetoelastic coupling, and antisymmetric exchange leading to the magnetoelectric effect. In our previous work (Ref. 13, hereafter referred to as I), the observation of the field-induced sequence of period-4 (P4), IC, period-5 (P5), and P3 basal-plane modulated spin structures at $T=0$ was shown to be a consequence of competition among these disparate interactions. As the temperature is lowered in zero applied field, CuFeO_2 exhibits successive magnetic transitions at $T_{N1} \approx 14$ K to a collinear IC state followed by a discontinuous transition at $T_{N2} \approx 11$ K to a collinear P4 spin structure. A similar sequence of transitions has also been reported in the triangular antiferromagnets MnBr_2 and NaFeO_2 .^{14,15}

In the present work, a representation of these effects is incorporated into a nonlocal Landau-type free-energy functional of the spin density $F[\mathbf{s}(\mathbf{r})]$ that is constructed from symmetry arguments in order to develop a model of the complex H - T phase diagram.¹⁰ The formalism is essentially phe-

nomenological but contains the same type of $T=0$ interactions that are considered in usual spin Hamiltonians. In the case of CuFeO_2 , these include in-plane exchange interactions up to third neighbor J_1 , J_2 , and J_3 (Refs. 16–19) as well as interplane exchange J' .^{7,19,20} These interactions lead to a minimization of the wave-vector-dependent exchange interaction $J_{\mathbf{Q}}$ near a multicritical point where multiple periodicities are close in energy. In addition to various biquadratic exchange interactions (symmetric and antisymmetric) and usual axial anisotropy, the rhombohedral $R\bar{3}m$ crystal symmetry also allows for the existence of an unusual trigonal interaction which was previously used to explain the magnetic structure anomalies in pure Ho.²¹ The importance of this term in stabilizing canted structures is explored here. This formalism also leads to umklaplike terms in the free energy which are nonzero only if a multiple of the ordering wave vector is equal to a crystal reciprocal-lattice vector \mathbf{G} , i.e., $n\mathbf{Q}=\mathbf{G}$ with n having values of 3, 4, and 5 in the present case. Within the Landau formalism, these types of terms are then responsible for the stability of the commensurate phases depending on the values of T and H . A Landau-type expansion based on molecular-field theory applied to MnBr_2 is presented in Ref. 14, which contains features in common with the present model. A more formal group-theoretic approach to understand spin structures in a variety of multiferroic compounds, with a discussion of CuFeO_2 , is given in Ref. 22.

The nonlocal formalism naturally leads to fourth-order and higher contributions [in $\mathbf{s}(\mathbf{r})$] to the free energy which are dependent on \mathbf{Q} and illustrates explicitly that terms which are independently invariant (with respect to all symmetries) have independent coefficients.^{10,23} This contrasts with the usual *local* form of the Landau energy which results in all isotropic terms having the same coefficient at a given power of \mathbf{s} . From a phenomenological point of view, the strong symmetry arguments are sufficient to assign different values to each of the many coefficients. However, such nonlocal effects can also be understood to have microscopic origins by considering interactions between magnetic and other degrees of freedom, such as magnetoelastic coupling, which

gives rise to nonlocal biquadratic exchange terms. Spin-lattice coupling is known to be strong in CuFeO₂,^{13,24–26} which provides further justification for the present approach.

II. NONLOCAL LANDAU FREE ENERGY

The development here of a nonlocal Landau-type free-energy functional of the spin density $F[\mathbf{s}(\mathbf{r})]$ for CuFeO₂ follows the description given in Ref. 10 for triangular antiferromagnets and uses the symmetry arguments given in I. Although the expansion is carried out to sixth order, a number of simplifications can be made for the purpose of understanding the phase diagram. It is convenient to write our model for F as the sum of isotropic and anisotropic contributions in the form

$$F = F_2 + F_4 + F_6 + F_z + F_{\text{CP}} + F_K - \mathbf{m} \cdot \mathbf{H}, \quad (1)$$

where the first three terms are the isotropic contributions relevant for all magnetic systems

$$F_2 = \frac{1}{2V^2} \int d\mathbf{r}d\mathbf{r}' A(\mathbf{r} - \mathbf{r}') \mathbf{s}(\mathbf{r}) \cdot \mathbf{s}(\mathbf{r}'), \quad (2)$$

$$F_4 = \frac{1}{4V^4} \int d\mathbf{r}_1 d\mathbf{r}_2 d\mathbf{r}_3 d\mathbf{r}_4 B(\mathbf{r}_1, \mathbf{r}_2, \mathbf{r}_3, \mathbf{r}_4) [\mathbf{s}(\mathbf{r}_1) \cdot \mathbf{s}(\mathbf{r}_2)] \times [\mathbf{s}(\mathbf{r}_3) \cdot \mathbf{s}(\mathbf{r}_4)], \quad (3)$$

$$F_6 = \frac{1}{6V^6} \int d\mathbf{r}_1 \cdots d\mathbf{r}_6 C(\mathbf{r}_1, \dots, \mathbf{r}_6) [\mathbf{s}(\mathbf{r}_1) \cdot \mathbf{s}(\mathbf{r}_2)] [\mathbf{s}(\mathbf{r}_3) \cdot \mathbf{s}(\mathbf{r}_4)] \times [\mathbf{s}(\mathbf{r}_5) \cdot \mathbf{s}(\mathbf{r}_6)]. \quad (4)$$

Temperature dependence enters in the usual Landau treatment of the isotropic second-order term. Here it is generalized to be of the form

$$A(\mathbf{r}) = ak_B T \delta(\mathbf{r}) + j^2 J(\mathbf{r}), \quad (5)$$

where a depends on the total angular-momentum number j and $J(\mathbf{r})$ is the exchange interaction. Such a form can be derived from a molecular-field treatment of the corresponding Heisenberg Hamiltonian.^{14,27,28} This mean-field treatment also yields local forms for the higher-order isotropic terms, involving constants B and C , which also depend on j and are proportional to $k_B T$. The nonlocal form of spin interactions, such as biquadratic exchange, can arise from a variety of n -body interactions²⁹ or indirectly from the coupling of $\mathbf{s}(\mathbf{r})$ to other relevant degrees of freedom such as lattice or electronic (see the F_{CP} term below). Nonlocal fourth-order contributions to the energy of the form given above that arise from magnetoelastic coupling have been derived.^{28,30} In the present model, we set $k_B \equiv 1$ and $j \equiv 1$ and simply treat a and the nonlocal fourth- and sixth-order coefficients as phenomenological parameters of undefined microscopic origin but with the support for their existence in CuFeO₂ from the strong spin-lattice coupling and a nontrivial spin-polarized electronic structure.³¹

There are a large number of independent anisotropic contributions invariant with respect to the $R\bar{3}m$ crystal rhombo-

hedral symmetry group generators $\{S_6|000\}$ and $\{\sigma_v|000\}$.³² Only the essential terms are considered here. Axial anisotropy ($\hat{\mathbf{z}} \parallel \hat{\mathbf{c}}$) is included only at second order in s ;

$$F_z = \frac{1}{2V^2} \int d\mathbf{r}d\mathbf{r}' J_z(\mathbf{r} - \mathbf{r}') s_z(\mathbf{r}) s_z(\mathbf{r}'). \quad (6)$$

Note that although this general form includes both single-ion anisotropy D , where $\mathbf{r} = \mathbf{r}'$, as well as two-site anisotropic exchange, the model used in I which includes only the latter is adopted here. Since the anisotropy is small, such a distinction has little impact on the results presented below. Higher-order terms such as $(\mathbf{s} \cdot \mathbf{s}) s_z^2$ and s_z^4 are omitted here for simplicity.

The stability of the field-induced noncollinear phase at zero temperature was shown in I to be a result of including a biquadratic antisymmetric exchange term of the form

$$F_{\text{CP}} = -\frac{1}{8V^2 A_p} \sum_{\alpha} \int d\mathbf{r}d\mathbf{r}' \{C(\boldsymbol{\tau}) \hat{\boldsymbol{\tau}}^{\alpha} [\mathbf{s}(\mathbf{r}) \times \mathbf{s}(\mathbf{r}')] \cdot \hat{\mathbf{z}}\}^2, \quad (7)$$

where $\boldsymbol{\tau} = \mathbf{r} - \mathbf{r}'$ and $\alpha = x, y$. Such a term is invariant with respect to all relevant symmetries and therefore must exist in the energy. Contributions to it can also arise as a result of coupling between the electric polarization and lattice and spin vectors in the form³

$$F_C = \frac{1}{2V^2} \int d\mathbf{r}d\mathbf{r}' C(\boldsymbol{\tau}) [\mathbf{P}(\boldsymbol{\tau}) \times \hat{\boldsymbol{\tau}}] \cdot [\mathbf{s}(\mathbf{r}) \times \mathbf{s}(\mathbf{r}')]_z \quad (8)$$

in combination with the lowest-order contribution to F in \mathbf{P} given by^{33,34} $F_P = \frac{1}{2V^2} A_p \int d\mathbf{r}d\mathbf{r}' P(\boldsymbol{\tau})^2$. Such cross product interactions are known to stabilize helically polarized spin structures.³⁵ Further analysis of the dependence of \mathbf{P} on $\mathbf{s}(\mathbf{r})$ is given in Sec. III.

Systems with trigonal symmetry also support an unusual anisotropy term which couples in-plane and out-of-plane components of the spin vector.²¹ For simplicity we use the local single-site expression of this effect with a coefficient K ,

$$F_K = \frac{K}{2V} \int d\mathbf{r} s_z(\mathbf{r}) s_y(\mathbf{r}) [3s_x^2(\mathbf{r}) - s_y^2(\mathbf{r})]. \quad (9)$$

This interaction favors linear spin configurations, which are canted, having both z and basal-plane components. The combination of F_{CP} and F_K contributions to the free energy thus favor a canted elliptically polarized state which induces an electric polarization \mathbf{P} in the basal plane.

Trigonal anisotropy terms of this type have been linked to weak ferromagnetism in general and have provided a crucial mechanism for the understanding of the distortion of helical spin structures and wave vector lock-in phenomena in hexagonal rare-earth antiferromagnets.²¹ In these cases, it has been speculated that such an interaction could arise from spin-orbit coupling of band electrons. Although there has been some electronic structure calculations of the spin states in the present $3d^5$ semiconductor,³¹ a microscopic theory of a spin Hamiltonian appropriate for CuFeO₂ has not yet been developed.³⁶

III. WAVE-VECTOR REPRESENTATION

Positions within the rhombohedral lattice of the Fe^{3+} magnetic ions are described here through an equivalent simple hexagonal unit cell with three triangular layers A , B , and C using basis vectors $\mathbf{w}_A=0$, $\mathbf{w}_B=\frac{1}{2}a\hat{\mathbf{x}}+\frac{1}{3}b\hat{\mathbf{y}}+\frac{1}{3}c\hat{\mathbf{z}}$, and $\mathbf{w}_C=\frac{1}{2}a\hat{\mathbf{x}}-\frac{1}{3}b\hat{\mathbf{y}}-\frac{1}{3}c\hat{\mathbf{z}}$ with a and c being the lattice constants; $b=(\sqrt{3}/2)a$ and $\hat{\mathbf{x}}\perp\hat{\mathbf{y}}\perp\hat{\mathbf{z}}$. As discussed previously,^{10,14,28} long-range magnetic order is characterized by the function $\boldsymbol{\rho}(\mathbf{r})$ through the spin density written as

$$\mathbf{s}(\mathbf{r}) = \frac{V}{N} \sum_{\mathbf{R}_1} \sum_j \boldsymbol{\rho}_j(\mathbf{r}) \delta(\mathbf{r} - \mathbf{R}), \quad (10)$$

where $\mathbf{R}=\mathbf{R}_1+\mathbf{w}_j$; $\mathbf{R}_1=(n+\frac{1}{2}m)a\hat{\mathbf{x}}+mb\hat{\mathbf{y}}$ (with n and m being integers) specifies hexagonal Bravais lattice sites; $j=A,B,C$; and $N=3N_j$ is the number of magnetic ions. The variety of spin structures in the magnetic phase diagram of CuFeO_3 can be adequately distinguished with $\boldsymbol{\rho}$ expressed as a Fourier expansion with a small number of terms in the form

$$\boldsymbol{\rho}_j(\mathbf{r}) = \mathbf{m} + \mathbf{S}_j e^{i\mathbf{Q}\cdot\mathbf{r}} + \mathbf{S}_j^* e^{-i\mathbf{Q}\cdot\mathbf{r}}, \quad (11)$$

where \mathbf{m} is the uniform magnetization induced by an applied field along the $\hat{\mathbf{z}}$ axis, \mathbf{S} is the spin-polarization vector, and \mathbf{Q} is the primary wave vector. A full description of some of the ordered states requires additional Fourier components as discussed below.

With only near-neighbor coupling J' between planes, a reasonable *ansatz* is to assume that the complex spin-polarization vectors \mathbf{S}_j on adjacent layers differ only by a simple phase factor ϕ with each layer having an overall phase factor γ in the form²⁸

$$\mathbf{S}_A = \mathbf{S} e^{i\gamma}, \quad \mathbf{S}_B = \mathbf{S}_C = \mathbf{S} e^{i(\gamma-\phi)}. \quad (12)$$

The primary description of the spin polarization of each state is further characterized by writing⁹

$$\mathbf{S} = \mathbf{S}_1 + i\mathbf{S}_2, \quad (13)$$

where \mathbf{S}_1 and \mathbf{S}_2 are real vectors. Previous analysis of Landau-type models to describe the magnetic states of frustrated triangular antiferromagnets⁹⁻¹² has demonstrated that sufficient flexibility can be achieved by assuming that \mathbf{S}_1 and \mathbf{S}_2 are characterized by writing

$$\mathbf{S}_1 = S \cos \beta (\sin \theta \hat{\boldsymbol{\rho}}_1 + \cos \theta \hat{\mathbf{z}}), \quad \mathbf{S}_2 = S \sin \beta \hat{\boldsymbol{\rho}}_2, \quad (14)$$

where $\hat{\boldsymbol{\rho}}_1 \perp \hat{\boldsymbol{\rho}}_2 \perp \hat{\mathbf{z}}$, i.e., $\hat{\boldsymbol{\rho}}_1$ and $\hat{\boldsymbol{\rho}}_2$ are in the hexagonal basal plane. The Q th component of the spin density on layer A is then given by

$$s_A(\mathbf{r}) = 2\mathbf{S}_1 \cos(\mathbf{Q} \cdot \mathbf{r} + \gamma) - 2\mathbf{S}_2 \sin(\mathbf{Q} \cdot \mathbf{r} + \gamma). \quad (15)$$

Linearly polarized states are described with $\mathbf{S}_2=0$, proper helically polarized spin configurations are realized by $\mathbf{S}_1 \perp \mathbf{S}_2 \perp \mathbf{Q}$ with $S_1=S_2$ ($\beta=\pi/4$), and elliptically polarized states have $S_1 \neq S_2 \neq 0$. It is also convenient to define dimensionless wave vectors in units of the lattice constants

$$q_x = aQ_x, \quad q_y = bQ_y, \quad q_z = cQ_z. \quad (16)$$

The zero-field $\uparrow\uparrow\downarrow\downarrow$ P4 phase described in Fig. 11 of Ref. 16 for a single layer is characterized by the above relations with

$q_x=\pi$ and $q_y=0$ or equivalently $q_x=\pi/2$ and $q_y=3\pi/4$ due to the triangular symmetry, along with $\beta=0$, $\theta=0$, and $\gamma=\pi/4$ (also, see Ref. 14). In terms of triangular lattice basis vectors $\mathbf{a}=a\hat{\mathbf{x}}$ and $\mathbf{b}=\frac{1}{2}a\hat{\mathbf{x}}+b\hat{\mathbf{y}}$, the relations are $q_a=q_x$ and $q_b=\frac{1}{2}q_x+q_y$. Thus, for example, the above degenerate modulations are also described by $q_a=\pi$ and $q_b=\pi/2$, and by $q_a=\pi/2$ and $q_b=\pi$.

A. Second-order isotropic terms

The free-energy density as a function of \mathbf{m} , \mathbf{S} , and \mathbf{Q} is developed by using the spin density given by Eqs. (10) and (11) in expressions (1)–(9). As shown previously,^{10,28} this analysis naturally leads to umklapp terms arising from the condition for periodic lattices

$$\frac{1}{N_l} \sum_{\mathbf{R}_l} e^{i\mathbf{n}\cdot\mathbf{Q}\cdot\mathbf{R}_l} = \Delta_{\mathbf{n}\cdot\mathbf{Q},\mathbf{G}}, \quad (17)$$

where \mathbf{G} is a hexagonal reciprocal-lattice vector. Second-order isotropic contributions reduce to

$$F_2 = \frac{1}{2} A_0 m^2 + A_{\mathbf{Q}} S^2, \quad (18)$$

where $S^2 = \mathbf{S} \cdot \mathbf{S}^*$, $A_{\mathbf{Q}} = aT + J_{\mathbf{Q}}$, and

$$J_{\mathbf{Q}} = \frac{1}{N} \sum_{\mathbf{R}} J(\mathbf{R}) e^{i\mathbf{Q}\cdot\mathbf{R}}. \quad (19)$$

Within the present model, this leads to the following wave-vector dependence of the exchange integral $J_{\mathbf{Q}} = 2f(\mathbf{q}, \phi)$ with

$$f(\mathbf{q}, \phi) = J_1 f_1(\mathbf{q}) + J_2 f_2(\mathbf{q}) + J_3 f_3(\mathbf{q}) + \frac{1}{3} J' f'(\mathbf{q}) (1 + 2 \cos \phi), \quad (20)$$

where³⁷

$$f_1 = \cos q_x + 2 \cos \frac{1}{2} q_x \cos q_y,$$

$$f_2 = \cos 2q_y + 2 \cos \frac{3}{2} q_x \cos q_y,$$

$$f_3 = \cos 2q_x + 2 \cos q_x \cos 2q_y,$$

$$f' = \cos \left(\frac{2}{3} q_x - \frac{1}{3} q_z \right) + 2 \cos \frac{1}{2} q_x \cos \left(\frac{1}{3} q_y + \frac{1}{3} q_z \right), \quad (21)$$

and $J_1=J(a\hat{\mathbf{x}})$, $J_2=J(2b\hat{\mathbf{y}})$, $J_3=J(2a\hat{\mathbf{x}})$, and $J'=J(\mathbf{w})$. Note that $J_i > 0$ represents antiferromagnetic coupling. Using these results, the coefficient of m^2 can be expressed as $A_0 = aT + 2f(0,0)$.

Within this mean-field theory, the wave vector characterizing the first ordered phase, to appear as the temperature is lowered from the paramagnetic state ($S=0$), is determined by the extrema of $J_{\mathbf{Q}}$ (the effects of anisotropic exchange are discussed below). Results of a numerical algorithm sketching

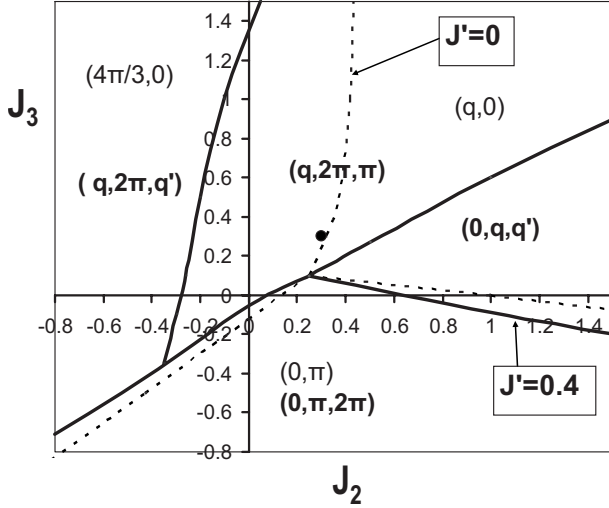


FIG. 1. Sketch of the J_2 - J_3 phase diagram based on minimization of the exchange integral J_q with $J_1=1$. Broken curves correspond to the case $J'=0$ and solid curves to $J'=0.4$. Solid circle indicates values used in the present model; $J_2=J_3=0.3$ and $J'=0.4$.

the J_2 - J_3 phase diagram are shown in Fig. 1 (also, see Ref. 37). Here, we set $J_1=1$ for convenience and consider two values of interlayer coupling, $J'=0$ and 0.4 , as in I. In the case of $J'=0$ (broken lines), the usual P3 modulation found in the frustrated triangular antiferromagnet (associated with, for example, 120° spin structures) occurs in the upper left part of the diagram. At more positive values of J_2 , further frustration stabilizes an IC modulation. Simple antiferromagnetic structures¹⁶ (P2) are found in the lower right region. Note that due to the triangular symmetry, there are a number of equivalent wave-vector descriptions for the same basic structure. For example, 120° spin configurations with $(4\pi/3, 0)$ and $(2\pi/3, \pi)$ differ only in their chirality.¹⁰ Period-2 structures with $(0, \pi)$, $(2\pi, 0)$, and $(\pi, \pi/2)$ differ only by a rotation of axes. With the addition of interlayer exchange $J'=0.4$ (solid lines), there is a nontrivial interplay between q_z and q_x, q_y as can be seen in Eq. (21). The boundary between P3 and IC phases disappears and there is an additional AF or IC modulation between adjacent planes. For example, in the lower part of the phase diagram, degenerate modulations $(0, \pi, 2\pi)$ and $(2\pi, 0, 0)$ both yield simple AF interplane structures since $\mathbf{q} \cdot \mathbf{w}_B = \pi$ and $\mathbf{q} \cdot \mathbf{w}_C = \pi$. Also indicated on Fig. 1 is the point corresponding to $J_2=0.3$ and $J_3=0.3$ (close to the values in I) which are used in the calculation of the H - T phase diagram described below.

B. Fourth- and sixth-order isotropic terms

Higher-order terms can also be evaluated with the assumed spin density (10)–(12). For convenience, regular (nonumklapp) terms and umklapp terms are written separately. In the case of the isotropic fourth-order contributions, the result can be expressed as follows:

$$F_4 = F_{4,R} + F_{4,3} + F_{4,4}, \quad (22)$$

where

$$F_{4,R} = B_1 S^4 + \frac{1}{2} B_2 |\mathbf{S} \cdot \mathbf{S}|^2 + \frac{1}{4} B_3 m^4 + 2B_4 |\mathbf{m} \cdot \mathbf{S}|^2 + B_5 m^2 S^2, \quad (23)$$

$$F_{4,3} = B_{4,3} [(\mathbf{m} \cdot \mathbf{S})(\mathbf{S} \cdot \mathbf{S})e^{3i\gamma} + \text{c.c.}] \Delta_{3\mathbf{Q},\mathbf{G}}, \quad (24)$$

$$F_{4,4} = \frac{1}{4} B_{4,4} [(\mathbf{S} \cdot \mathbf{S})^2 e^{4i\gamma} + \text{c.c.}] \Delta_{4\mathbf{Q},\mathbf{G}}. \quad (25)$$

As shown in Ref. 10, umklapp terms involving $2\mathbf{Q}$ are accounted for within the regular terms by a suitable renormalization of the spin-density amplitude. Expressions for some of the coefficients in terms of the Fourier transform of the nonlocal function $B(\mathbf{r}_1, \mathbf{r}_2, \mathbf{r}_3, \mathbf{r}_4)$ are given in Ref. 10 and the others may be easily deduced. For example, $B_1 = B_{\mathbf{Q},-\mathbf{Q},\mathbf{Q},-\mathbf{Q}}$, $B_4 = B_{0,\mathbf{Q},0,-\mathbf{Q}}$, and $B_{4,3} = B_{0,\mathbf{Q},\mathbf{Q},\mathbf{Q}}$. The important point here is that the nonlocal formulation naturally leads to the result that each independently invariant term has its own independent coefficient. In a local formulation, all isotropic terms have equal coefficients. In the present model, each of these fourth-order (and sixth-order) independent coefficients is assumed to be constant. As discussed previously,^{9,23} noncollinear spin structures are stabilized with $B_2 > 0$ and collinear states with $B_2 < 0$. Usual spin-flop transitions in antiferromagnets occur as a consequence of having $B_4 > 0$ so that a spin configuration with $\mathbf{S} \perp \mathbf{H}$ is stabilized.

The above umklapp terms are nonzero only if $3\mathbf{Q}=\mathbf{G}$ (and $m \neq 0$) or $4\mathbf{Q}=\mathbf{G}$, allowing for the possibility of energy reduction if the system assumes these periodicities.¹⁴ In the case of $\mathbf{S} \parallel \mathbf{m}$ for the first term, or in the case of any collinear state for the second term, these expressions reduce to $2B_{4,3}mS^3 \cos(3\gamma)$ and $\frac{1}{2}B_{4,4}S^4 \cos(4\gamma)$, respectively. For positive coefficients, these two terms are then each minimized by phase factors $\gamma = \pi/3$ and $\pi/4$, respectively.

In an effort to reduce the number of model parameters, a somewhat simplified approach is adopted to treat the isotropic sixth-order contributions. In addition to the regular terms, there are umklapp terms involving periodicities $\mathbf{G}/3$, $\mathbf{G}/4$, $\mathbf{G}/5$, and $\mathbf{G}/6$. For simplicity, it is assumed that each of the independent terms forming the regular part has the same coefficient C . This is equivalent to a local formulation of these contributions. Each of the umklapp terms, however, are assigned an independent coefficient. The result can be expressed as

$$F_6 = F_{6,R} + F_{6,3} + F_{6,4} + F_{6,5} + F_{6,6}, \quad (26)$$

where

$$F_{6,R} = \frac{1}{6} C \{ S_T^6 + 6S_T^2 |\mathbf{S} \cdot \mathbf{S}|^2 + 24S_T^2 |\mathbf{m} \cdot \mathbf{S}|^2 + 12[(\mathbf{S} \cdot \mathbf{S})(\mathbf{m} \cdot \mathbf{S}^*)^2 + \text{c.c.}] \}, \quad (27)$$

$$F_{6,3} = \frac{1}{6} C_{6,3} \{ [12S_T^2 (\mathbf{m} \cdot \mathbf{S})(\mathbf{S} \cdot \mathbf{S}) + 6(\mathbf{m} \cdot \mathbf{S}^*)(\mathbf{S} \cdot \mathbf{S})^2 + 8(\mathbf{m} \cdot \mathbf{S})^3] e^{3i\gamma} + \text{c.c.} \} \Delta_{3\mathbf{Q},\mathbf{G}}, \quad (28)$$

$$F_{6,4} = \frac{1}{6} C_{6,4} \{ [3S_7^2(\mathbf{S} \cdot \mathbf{S})^2 + 20(\mathbf{m} \cdot \mathbf{S})^2(\mathbf{S} \cdot \mathbf{S})] e^{4i\gamma} + \text{c.c.} \} \Delta_{4\mathbf{Q},\mathbf{G}}, \quad (29)$$

$$F_{6,5} = C_{6,5} \{ (\mathbf{m} \cdot \mathbf{S})(\mathbf{S} \cdot \mathbf{S})^2 e^{5i\gamma} + \text{c.c.} \} \Delta_{5\mathbf{Q},\mathbf{G}}, \quad (30)$$

$$F_{6,6} = \frac{1}{6} C_{6,6} \{ (\mathbf{S} \cdot \mathbf{S})^3 e^{6i\gamma} + \text{c.c.} \} \Delta_{6\mathbf{Q},\mathbf{G}}. \quad (31)$$

Note that odd-order umklapp terms occur only in the presence of a magnetic field where $m \neq 0$ and have a maximum effect on lowering the free energy with linearly polarized spin configurations and $\mathbf{S} \parallel \mathbf{H}$. In-plane and c -axis periodicities, n and m , respectively, can be separated by writing $\mathbf{Q} = \frac{1}{n}\mathbf{G}_\perp + \frac{1}{m}\mathbf{G}_\parallel$, where \mathbf{G}_\perp and \mathbf{G}_\parallel are reciprocal-lattice vectors perpendicular and parallel to the hexagonal c axis. At low values of magnetic field, antiferromagnetic interplane exchange $J' > 0$ dominates and period-2 interlayer c axis modulations are stabilized. For the odd-period in-plane commensurate structures $\mathbf{Q}_\parallel = \mathbf{0}$, \mathbf{G}_\parallel and the umklapp conditions $3\mathbf{Q} = \mathbf{G}$ and $5\mathbf{Q} = \mathbf{G}$ are satisfied for P3 and P5 spin configurations, respectively. These characterizations are consistent with neutron-diffraction data.^{1,2}

A complete description of the spin structures usually requires that additional wave-vector components (\mathbf{Q}') be added to the Fourier expansion of the spin density (11) which lead to a “squaring up” of magnetic structures.^{12,14} Fourth-order isotropic umklapp terms of the form $(\mathbf{S}' \cdot \mathbf{S})(\mathbf{S} \cdot \mathbf{S})$ exist for cases where $\mathbf{Q}' + 3\mathbf{Q} = \mathbf{G}$ leading to the incipient relation $\mathbf{S}' \sim \mathbf{S}(\mathbf{S} \cdot \mathbf{S})$. With a magnetic field present, terms of the form $(\mathbf{S}' \cdot \mathbf{m})(\mathbf{S} \cdot \mathbf{S})$ occur at fourth order if $\mathbf{Q}' + 2\mathbf{Q} = \mathbf{G}$ giving $\mathbf{S}' \sim \mathbf{m}(\mathbf{S} \cdot \mathbf{S})$. A larger number of possible secondary wave vectors arise from sixth-order umklapp terms. A fully consistent analysis would lead to many additional contributions to the free energy, but it is not required for the semiquantitative description of the phase diagram given here.

C. Anisotropic terms

Evaluating the anisotropic contributions to the free energies F_z , F_{CP} , and F_K in terms of the spin-density parameters \mathbf{m} , \mathbf{S} , and \mathbf{Q} follows the method as described above. Since anisotropy is known to be small in CuFeO_2 , anisotropic umklapp terms are omitted for simplicity. The resulting anisotropic exchange terms are identical in form to isotropic exchange but involve only z components of the spin vectors;

$$F_z = \frac{1}{2} J_{z0} m_z^2 + J_{zQ} |S_z|^2. \quad (32)$$

Here, J_{zQ} is given by the relations (19)–(21) but with the isotropic exchange parameters J_i and J' replaced by their anisotropic counterparts J_{zi} and J'_z , as in I. The coefficient J_{z0} is then given by this expression evaluated at $\mathbf{Q} = \mathbf{0}$ and $\phi = 0$ in Eq. (21).

An expression for the nonlocal biquadratic antisymmetric exchange interaction can be determined by first evaluating F_C using Eqs. (10) and (11) with the assumption that the electric polarization vector \mathbf{P} is uniform. This gives³⁸

$$F_C = i(C_x P_x + C_y P_y) \hat{\mathbf{z}} \cdot (\mathbf{S} \times \mathbf{S}^*), \quad (33)$$

where, as in I, magnetoelectriclike interactions $C_1 = C(a\hat{\mathbf{x}})$ and $C' = C(\mathbf{w})$ are included, giving

$$C_x = -\frac{4}{3}b \left\{ C_1 \cos \frac{1}{2} q_x \sin q_y - \frac{1}{3} C' \left[\sin \left(\frac{1}{3} q_z - \frac{2}{3} q_y \right) - \sin \left(\frac{1}{3} q_x + \frac{1}{3} q_y \right) \cos \frac{1}{2} q_x \right] (1 + 2 \cos \phi) \right\},$$

$$C_y = \frac{2}{3}a \left\{ C_1 \left(\sin q_x + \sin \frac{1}{2} q_x \cos q_y \right) + C' \sin \frac{1}{2} q_x \cos \left(\frac{1}{3} q_y + \frac{1}{3} q_z \right) (1 + 2 \cos \phi) \right\}. \quad (34)$$

Minimization of the free energy $F_{CP} = F_C + F_P$, where $F_P = \frac{1}{2} A_P (P_x^2 + P_y^2)$, thus yields the relations between \mathbf{P} and the spin-polarization vectors;

$$P_x = -(i/A_P) C_x (\mathbf{S} \times \mathbf{S}^*)_z,$$

$$P_y = -(i/A_P) C_y (\mathbf{S} \times \mathbf{S}^*)_z. \quad (35)$$

The combined antisymmetric biquadratic exchange contribution to the free energy then takes the form

$$F_{CP} = \frac{1}{2A_P} (C_x^2 + C_y^2) (\mathbf{S} \times \mathbf{S}^*)_z^2. \quad (36)$$

These relations make clear that a uniform electric polarization cannot be induced by a collinear spin structure where $\beta = 0$ or $\pi/2$ since

$$(\mathbf{S} \times \mathbf{S}^*)_z = 2i(\mathbf{S}_1 \times \mathbf{S}_2)_z = iS^2 \sin 2\beta \sin \theta. \quad (37)$$

Note also that $\mathbf{P} = \mathbf{0}$ in cases where \mathbf{S} lies strictly in the $\hat{\mathbf{z}}\text{-}\hat{\rho}_2$ plane ($\theta = 0$) as has been recently emphasized.^{5,20,39,40}

Finally, the local formulation of the trigonal anisotropy term given above can be expressed in terms of the spin-polarization vector components as

$$F_K = K \{ [3(S_x^*)^2 S_y S_z - S_z S_y (S_y^*)^2 + 2S_y S_z^* (3|S_x|^2 - |S_y|^2)] + \text{c.c.} \}. \quad (38)$$

Using the parametrizations of \mathbf{S} given above, this interaction term can be written as

$$F_K = 3KS^4 \cos^2 \beta \sin 2\theta (\sin^2 \beta - \cos^2 \beta \sin^2 \theta), \quad (39)$$

which generally favors canted spin structures $0 < \theta < \pi/2$.

IV. MAGNETIC PHASE DIAGRAM OF CuFeO_2

The nonlocal free-energy functional formulated above can be expressed as a function of the parameters which characterize the spin density $F = F(\mathbf{Q}, S, m, \phi, \gamma, \theta, \beta)$. Equilibrium spin configurations as a function of temperature and magnetic field are then determined by minimization (numerically) of F for a given set of coefficients. Since the phase diagram involves spin structures characterized by a number of different wave vectors \mathbf{Q} , which can each have associated

umklapp terms, it is necessary to minimize (with respect to the other parameters) separately and compare the distinct free energies associated with IC, $3\mathbf{Q}=\mathbf{G}$, $4\mathbf{Q}=\mathbf{G}$, and $5\mathbf{Q}=\mathbf{G}$ (labeled $F_{IC}, F_{P3}, F_{P4}, F_{P5}$) phases in order to determine the equilibrium state.

A feature of the present model is the large number of coefficients which is a consequence of not only the nonlocal formulation but also the many competing interactions. This multitude of effects are, however, essential for a complete understanding of the complex magnetic phase diagram of this highly frustrated compound. In order to reduce the number of free parameters, zero-temperature coefficient values from I are used here and other coefficients are *a priori* assigned reasonable values. Only a relatively small number of coefficients are adjusted in an effort to reproduce the essential features of the phase diagram. As in I, the overall energy scale is set by assigning $J_1 \equiv 1$ with other exchange parameters given by $J_2=J_3=0.3$ and $J'=0.4$. Magnetoelectric coupling coefficients used in I are adopted here, $C_1=0.3$, $C'=0.1$, and $A_p=1$, as well as the assignment of an anisotropy strength of 3% so that $J_{iz}=0.03J_i$ and $J'_z=0.03J'$. This level of anisotropy is also adopted here for the trigonal coefficient $K=0.03$. Some of the Landau coefficients were arbitrarily set as follows: $a=1$, $B_0=1$, $B_1=1$, $B_2=0.1$, $B_3=0.1$, and $C=0.1$. Assuming a positive value for the term $B_4|\mathbf{m}\cdot\mathbf{S}|^2$ was always found to yield a low-field spin-flop transition (since anisotropy is weak), which is not observed in the magnetic phase diagram of CuFeO_2 (at least in moderate field values). Assigning the negative value $B_4=-0.2$ serves to enhance the stability of the reported configurations with $\mathbf{S}\parallel\mathbf{H}$ in the P5 and P3 states (also, see Ref. 11). (This point is discussed further below.) Coefficients of the umklapp terms $B_{4,3}$, $B_{4,4}$, $C_{6,6} \equiv C_{6,3}$, $C_{6,4}$, and $C_{6,5}$ are then adjusted to reproduce essential features of the H - T phase diagram. Note that the $6\mathbf{Q}=\mathbf{G}$ umklapp term in Eq. (31) contributes to the P3 state and its coefficient is assigned the same value as the sixth-order $3\mathbf{Q}=\mathbf{G}$ umklapp term for simplicity.

For the range of coefficients considered here, the interlayer phase factor ϕ is always found to be zero. The overall spin-polarization phase factor γ appears only in umklapp terms and the free energy is minimized with $\gamma=\pi/n$ for commensurate states described by $n\mathbf{Q}=\mathbf{G}$.

Consider first the sequence of transitions which occurs at $H=0$. With the addition of axial anisotropy, the spin structure to first appear as the temperature is lowered from the paramagnetic state, is linearly polarized $\mathbf{S}\parallel\hat{c}$. The free energy up to fourth order is given by

$$F_0 = (A_{\mathbf{Q}} + J_{z\mathbf{Q}})S^2 + \left(B_1 + \frac{1}{2}B_2\right)S^4 + \frac{1}{2}B_{4,4}S^4 \cos(4\gamma)\Delta_{4\mathbf{Q},\mathbf{G}} \quad (40)$$

with the transition temperature given by $T_{N1} = -(J_{\mathbf{Q}} + J_{z\mathbf{Q}})/a$. The wave vector is thus determined by the value which maximizes this function as shown in Fig. 1. For the set of exchange parameters used here, this gives the collinear IC phase with degenerate wave vectors $(q_x, q_y, q_z) = (2q, 2\pi, \pi)$, $(2\pi - q, 3/2q - \pi, \pi)$, and $(2\pi - 2q, \pi, \pi)$ [or equivalently $(q_a, q_b, q_c) = (2q, 2\pi + q, \pi)$, $(2\pi - q, q, \pi)$, and $(2\pi - 2q, 2\pi$

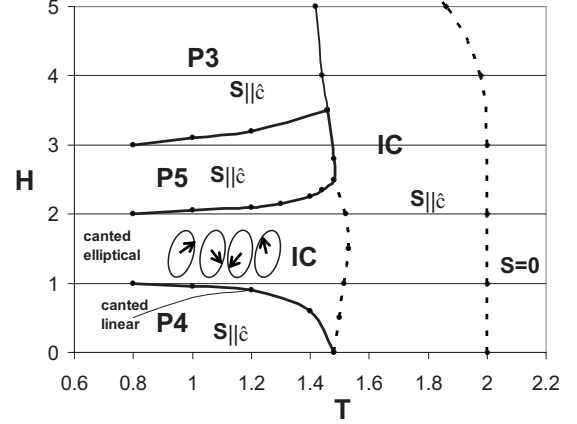


FIG. 2. Sketch of the model phase diagram based for CuFeO_2 on minimization of the free energy (in units of J_1). Solid and broken lines represent discontinuous and continuous transitions, respectively.

$-q, \pi)$, respectively] where $q \approx 0.22$, giving $T_{N1} \approx 2.0$. The result $\frac{1}{5} < q < \frac{1}{4}$ is consistent with neutron-diffraction data² and the speculation of multi- \mathbf{q} domain structures.⁴⁰ Numerical minimization of the free energies corresponding to IC and P4 $(\pi, 2\pi, \pi)$ phases with all terms included is then performed in order to compare F_{IC} and F_{P4} as a function of temperature.¹⁴ Assigning the parameter values $B_{4,4}=0.8$ and $C_{6,4}=0.2$ is found to yield the result $F_{P4} < F_{IC}$ for $T < T_{N2} \approx 1.5$, which approximately agrees with the experimental data for T_{N2}/T_{N1} . The transition at T_{N1} is continuous while the IC-P4 transition at T_{N2} is discontinuous.

Using this method of comparing free energies associated with IC and commensurate spin states, the phase diagram with $\mathbf{H}\parallel\hat{c}$ is determined numerically. The three remaining coefficients are fit to best reproduce the transition boundaries in an effort to achieve semiquantitative agreement with the corresponding experimental results presented in Refs. 3 and 4. This procedure yields $B_{4,3}=1.0$, $C_{6,6}=0.1$, and $C_{6,5}=0.6$. The linear IC, P5, and P3 phases remain stable with $\mathbf{S}\parallel\hat{c}$ at all field values considered due to setting $B_4 < 0$. The elliptical IC phase is stabilized at moderate field values with $\beta \approx 0.19\pi$ at lower T . There is little change in wave vector from the zero-field values since C_x^2 and C_y^2 in Eq. (36) are small. Due to the small trigonal interaction term F_K , this structure is also found to be canted away from the \hat{c} axis by about $\theta \approx 10^\circ$. Similarly, at low temperatures, the linear P4 phase exhibits a discontinuous transition to canting away from the \hat{c} axis by about 45° (indicated by the thin solid line in Fig. 2). The transition between elliptical and linear IC phases is continuous with β acting as an order parameter. The canting of magnetic structures does not occur within the present model in the case $K=0$. Critical fields at low temperature, $H_{P4-IC} \approx 1$, $H_{IC-P5} \approx 2$, $H_{P5-P3} \approx 3$, are in fair agreement with the experimentally observed ratios $H_{IC-P5}/H_{P4-IC} \approx 13T/7T$ and $H_{P5-P3}/H_{P4-IC} \approx 20T/7T$.^{3,4}

V. DISCUSSION AND CONCLUSIONS

In this work, a model nonlocal Landau-type free energy that captures essential features of the complex magnetic

phase diagram of the highly frustrated magnetoelectric triangular antiferromagnet CuFeO_2 and serves as an extension of a previous zero-temperature model¹³ has been developed and analyzed. In contrast to local formulations, the present approach naturally leads to the result that each symmetry-invariant isotropic term has its own independent coefficient. In the case of CuFeO_2 , it is argued that strong magnetoelastic coupling is one source for such nonlocal biquadratic (and higher-order) spin interactions. As emphasized in Ref. 13, magnetoelectric coupling also provides a microscopic mechanism for the existence of biquadratic antisymmetric exchange. In addition to weak axial anisotropy, the rhombohedral crystal symmetry also supports a somewhat unusual trigonal term which couples basal-plane and axial spin components. With analysis performed in terms of a Fourier expansion of the spin density, this approach also facilitates comparison with neutron-diffraction data.

There are a number of limitations associated with this method. The Landau model is an expansion of the free energy around $\mathbf{s}(\mathbf{r})=0$ so that results far below T_N and at high-field values may require a large number of terms. In addition, only a small number of modulated spin structures can be fully described by just a few Fourier components. The model in its present form fails, for example, to account for the very high-field spin-flop P3 phase suggested by magnetization measurements.⁴ The merging of P4, IC, and P5 transition boundaries suggested by the experimentally determined phase diagram is also not found in our truncated model. The reentrant behavior associated with this multicritical point⁶ is not a feature of the present Landau expansion. Alternative theoretical approaches could be useful for this purpose, such as those which do not rely on a restricted form of the Landau order-parameter function, but solutions can be difficult even in cases of relatively simple systems.⁴¹ In principle, the Hamiltonian associated with the free energy examined here could also be treated within a nonperturbative mean-field approach, a method which can be successful in producing more subtle aspects of phase diagrams in frustrated spin systems such as reentrant phenomena.⁴² Note that within the present (mean-field) formulation, the paramagnetic-IC (para-IC) transition temperature is given by $T_{N1} = -(J_Q + J_z \mathbf{Q})j^2 / (ak_B)$, where $a = 3/[2j(j+1)]$. Using $j = 5/2$ and the estimate $J_1 \approx 5.3K(k_B)$ from spin-wave data¹⁹ (along with the other exchange interactions values given above) gives $T_{N1} = 38.6K$. The nearly factor of 3 discrepancy with the experimental value can be attributed to strong critical fluctuation effects associated with the high degree of frustration in this compound.

The nature of the symmetry breaking at the two continuous transitions, para-IC and IC(linear)-IC(elliptical), can be analyzed in a manner similar to the weak axial triangular antiferromagnet CsNiCl_3 .⁴³ Both should belong to the stan-

dard XY universality class involving a two-component continuous order parameter. In the case of the para-IC transition, the two components can be identified as the magnitude of the spin order S and the associated phase angle γ . In the case of unfrustrated systems, this transition would be identified with Ising universality. In the finite-field transition to the elliptical phase, the system develops (XY) basal-plane components $\hat{\rho}_1$ and $\hat{\rho}_2$.

The consequence of the present model and analysis is that basal-plane components of the electric polarization \mathbf{P} are induced by the mechanism proposed by Kimura *et al.*³ if the spin structure is canted relative to the \hat{c} axis. This result offers a resolution to the issue raised recently concerning the microscopic origin of the magnetoelectric effect in this compound.^{5,20,39,40} Such a canting occurs in crystals with rhombohedral symmetry only as a consequence of the trigonal interaction term F_K .

The method and some of the results presented here are also relevant to other frustrated triangular antiferromagnets. Although hexagonal MnBr_2 shows planar anisotropy and strong interplane coupling responsible for a period-4 c -axis modulation, it shares the same basal-plane P4-IC transition as CuFeO_2 .¹⁴ NaFeO_2 not only has the same rhombohedral symmetry as CuFeO_2 and a P4-IC transition but also has $\mathbf{S} \perp \hat{c}$ and a more complicated P4 spin structure.¹⁵ Two of the three basal-plane triangular crystal directions show period-4 modulations and the third is ferromagnetic. This can be described by $\mathbf{q} = (\pi/2, \pi/4)_{xy}$ or equivalently $\mathbf{q} = (\pi/2, \pi/2)_{ab}$, which satisfy the umklapp requirement $4\mathbf{Q} = \mathbf{G}$. Differences with CuFeO_2 could be due to additional interplane exchange interactions. It is of interest to note that this material does not appear to exhibit the structural phase transition to monoclinic symmetry found in CuFeO_2 below T_{N1} , providing another example where the stability of a P4 phase is not related to a structural distortion. Other potential applications of the present model include the hexagonal magnetoelectric antiferromagnet $\text{RbFe}(\text{MoO}_4)_2$, which exhibits a complex phase diagram involving P3, P4, and P5 spin structures,⁴⁴ and a series of rhombohedral magnetoelectric antiferromagnets ACrO_2 ($A = \text{C}_r, \text{A}_g, \text{Li}, \text{and Na}$).⁴⁵ Even in cases of frustrated spin systems with relatively few interactions, enhanced understanding of finite temperature effects has been achieved by re-examination through successively less approximative models—Landau theory, mean-field theory, and, finally, Monte-Carlo simulations.¹² Application of these latter techniques to the complex phase diagrams of CuFeO_2 and related systems is desirable.

ACKNOWLEDGMENTS

I thank G. Quirion and M. J. Tagore for the enlightening discussions. This work was supported by the Natural Science and Engineering Research Council of Canada (NSERC).

- ¹O. A. Petrenko, G. Balakrishnan, M. R. Lees, D. McK. Paul, and A. Hoser, *Phys. Rev. B* **62**, 8983 (2000).
- ²S. Mitsuda, N. Kasahara, T. Uno, and M. Mase, *J. Phys. Soc. Jpn.* **67**, 4026 (1998); S. Mitsuda, M. Mase, K. Prokes, H. Kitazawa, and H. A. Katori, *ibid.* **69**, 3513 (2000).
- ³T. Kimura, J. C. Lashley, and A. P. Ramirez, *Phys. Rev. B* **73**, 220401(R) (2006).
- ⁴N. Terada, Y. Narumi, K. Katsumata, T. Yamamoto, U. Staub, K. Kindo, M. Hagiwara, Y. Tanaka, A. Kikkawa, H. Toyokawa, T. Fukui, R. Kanmuri, T. Ishikawa, and H. Kitamura, *Phys. Rev. B* **74**, 180404(R) (2006).
- ⁵T. Nakajima, S. Mitsuda, S. Kanetsuki, K. Prokes, A. Podlesnyak, H. Kimura, and Y. Noda, *J. Phys. Soc. Jpn.* **76**, 043709 (2007).
- ⁶S. Seki, Y. Yamasaki, Y. Shiomi, S. Iguchi, Y. Onose, and Y. Tokura, *Phys. Rev. B* **75**, 100403(R) (2007).
- ⁷O. A. Petrenko, M. R. Lees, G. Balakrishnan, S. de Brion, and G. Chouteau, *J. Phys.: Condens. Matter* **17**, 2741 (2005).
- ⁸M.-H. Whangbo, D. Dai, K.-S. Lee, and R. K. Kremer, *Chem. Mater.* **18**, 1268 (2006).
- ⁹M. L. Plumer, K. Hood, and A. Caillé, *Phys. Rev. Lett.* **60**, 45 (1988).
- ¹⁰M. L. Plumer and A. Caillé, *Phys. Rev. B* **37**, 7712 (1988).
- ¹¹M. L. Plumer, A. Caillé, and K. Hood, *Phys. Rev. B* **39**, 4489 (1989).
- ¹²M. L. Plumer, A. Caillé, A. Mailhot, and H. T. Diep, in *Magnetic Systems with Competing Interactions*, edited by H. T. Diep (World Scientific, Singapore, 1994).
- ¹³M. L. Plumer, *Phys. Rev. B* **76**, 144411 (2007).
- ¹⁴T. Sato, H. Kadowaki, H. Masuda, and K. Iio, *J. Phys. Soc. Jpn.* **63**, 4583 (1994); T. Sato, H. Kadowaki, and K. Iio, *Physica B* **213**, 224 (1995).
- ¹⁵T. McQueen, Q. Huang, J. W. Lynn, R. F. Berger, T. Klimczuk, B. G. Ueland, P. Schiffer, and R. J. Cava, *Phys. Rev. B* **76**, 024420 (2007).
- ¹⁶M. Mekata, N. Yaguchi, T. Takagi, T. Sugino, S. Mitsuda, H. Yoshizawa, N. Hosoito, and T. Shinjo, *J. Phys. Soc. Jpn.* **62**, 4474 (1993).
- ¹⁷Y. Ajiro, T. Asano, T. Takagi, M. Mekata, H. A. Katori, and T. Goto, *Physica B (Amsterdam)* **201**, 71 (1994).
- ¹⁸T. Fukuda, H. Nojiri, M. Motokawa, T. Asano, M. Mekata, and Y. Ajiro, *Physica B (Amsterdam)* **246-247**, 569 (1998).
- ¹⁹F. Ye, J. A. Fernandez-Baca, R. S. Fishman, Y. Ren, H. J. Kang, Y. Qiu, and T. Kimura, *Phys. Rev. Lett.* **99**, 157201 (2007).
- ²⁰N. Terada, S. Mitsuda, T. Fujii, and D. Petitgrand, *J. Phys.: Condens. Matter* **19**, 145241 (2007).
- ²¹T. Moriya, *Magnetism*, edited by G. T. Rado and H. Suhl (Academic, New York, 1963), Vol. 1; J. Jensen and A. R. MacKintosh, *Rare Earth Magnetism* (Clarendon, Oxford, 1991); R. A. Cowley and J. Jensen, *J. Phys.: Condens. Matter* **4**, 9673 (1992); J. A. Simpson, D. F. McMorrow, R. A. Cowley, and D. A. Jehan, *Phys. Rev. B* **51**, 16073 (1995); J. Jensen, *ibid.* **54**, 4021 (1996).
- ²²A. B. Harris, *Phys. Rev. B* **76**, 054447 (2007).
- ²³M. B. Walker, *Phys. Rev. B* **22**, 1338 (1980).
- ²⁴F. Ye, Y. Ren, Q. Huang, J. A. Fernandez-Baca, P. Dai, J. W. Lynn, and T. Kimura, *Phys. Rev. B* **73**, 220404(R) (2006); N. Terada, S. Mitsuda, H. Ohsumi, and K. Tajima, *J. Phys. Soc. Jpn.* **75**, 23602 (2006); N. Terada, Y. Narumi, Y. Sawai, K. Katsumata, U. Staub, Y. Tanaka, A. Kikkawa, T. Fukui, K. Kindo, T. Yamamoto, R. Kanmuri, M. Hagiwara, H. Toyokawa, T. Ishikawa, and H. Kitamura, *Phys. Rev. B* **75**, 224411 (2007); G. Quirion, M. J. Tagore, M. L. Plumer, and O. A. Petrenko, *ibid.* **77**, 094111 (2008).
- ²⁵N. Terada, S. Mitsuda, Y. Tanaka, Y. Tabata, K. Katsumata, and A. Kikkawa, *J. Phys. Soc. Jpn.* **77**, 054701 (2008).
- ²⁶F. Wang and A. Vishwanath, *Phys. Rev. Lett.* **100**, 077201 (2008).
- ²⁷P. Bak and J. von Boehm, *Phys. Rev. B* **21**, 5297 (1980).
- ²⁸M. L. Plumer, *Phys. Rev. B* **44**, 12376 (1991).
- ²⁹J. Adler and J. Oitmaa, *J. Phys. C* **12**, 575 (1979).
- ³⁰D. L. Bergman, R. Shindou, G. A. Fiete, and L. Balents, *Phys. Rev. B* **74**, 134409 (2006).
- ³¹V. R. Galakhov, A. I. Poteryaev, E. Z. Kurmaev, V. I. Anisimov, St. Bartkowski, M. Neumann, Z. W. Lu, B. M. Klein, and T.-R. Zhao, *Phys. Rev. B* **56**, 4584 (1997); V. Eyert, R. Frésard, and A. Maignan, arXiv:0801.4787 (unpublished).
- ³²C. J. Bradley and A. P. Cracknell, *The Mathematical Theory of Symmetry in Solids* (Clarendon, Oxford, 1972).
- ³³H. Katsura, N. Nagaosa, and A. V. Balatsky, *Phys. Rev. Lett.* **95**, 057205 (2005); H. Katsura, A. V. Balatsky, and N. Nagaosa, *ibid.* **98**, 027203 (2007).
- ³⁴A. V. Syromyatnikov, *JETP* **105**, 587 (2007).
- ³⁵I. E. Dzyaloshinskii, *Sov. Phys. JETP* **19**, 960 (1964).
- ³⁶S. Febbraro, *J. Phys. C* **20**, 5367 (1987); H. Yue and Y. Zi-Yuan, *J. Magn. Magn. Mater.* **299**, 445 (2006).
- ³⁷E. Rastelli, A. Tassi, and L. Reatto, *Physica B (Amsterdam)* **97**, 1 (1979); A. P. J. Jansen, *Phys. Rev. B* **33**, 6352 (1986); J. N. Reimers and J. R. Dahn, *J. Phys.: Condens. Matter* **4**, 8105 (1992).
- ³⁸M. L. Plumer, H. Kawamura, and A. Caillé, *Phys. Rev. B* **43**, 13786(R) (1991).
- ³⁹T. Arima, *J. Phys. Soc. Jpn.* **76**, 073702 (2007).
- ⁴⁰H. Mitamura, S. Mitsuda, S. Kanetsuki, H. A. Katori, T. Sakakibara, and K. Kindo, *J. Phys. Soc. Jpn.* **76**, 094709 (2007).
- ⁴¹See, for example, M. Krech, *Phys. Rev. E* **56**, 1642 (1997); E. Brézin and C. De Dominicis, *Eur. Phys. J. B* **24**, 353 (2001).
- ⁴²A. D. Beath and D. H. Ryan, *Phys. Rev. B* **72**, 014455 (2005).
- ⁴³H. Kawamura, A. Caillé, and M. L. Plumer, *Phys. Rev. B* **41**, 4416 (1990); G. Quirion, X. Han, M. L. Plumer, and M. Poirier, *Phys. Rev. Lett.* **97**, 077202 (2006).
- ⁴⁴M. Kenzelmann, G. Lawes, A. B. Harris, G. Gasparovic, C. Broholm, A. P. Ramirez, G. A. Jorge, M. Jaime, S. Park, Q. Huang, A. Ya. Shapiro, and L. A. Demianets, *Phys. Rev. Lett.* **98**, 267205 (2007); A. I. Smirnov, H. Yashiro, S. Kimura, M. Hagiwara, Y. Narumi, K. Kindo, A. Kikkawa, K. Katsumata, A. Ya. Shapiro, and L. N. Demianets, *Phys. Rev. B* **75**, 134412 (2007).
- ⁴⁵S. Seki, Y. Onose, and Y. Tokura, arXiv:0801.3757 (unpublished).